

# An RXTE Observation of the Vela Pulsar: Filling in the X-ray Gap

M.S. Strickman<sup>1</sup>

*Naval Research Laboratory*

A.K. Harding

*NASA Goddard Space Flight Center*

and

O.C. deJager

*Potchefstroom University*

## ABSTRACT

We have detected pulsed emission from the Vela pulsar at 2 - 30 keV during a 93 ks observation with the *Rossi X-Ray Timing Explorer* (RXTE). The RXTE pulse profile shows two peaks, that are roughly in phase with the EGRET peaks, but does not show any significant interpeak emission. The phase of Peak 2 is energy dependent, moving to higher phase with increasing energy in the RXTE band, in phase alignment with the second optical pulse in the lowest energy band of 2 - 8 keV and in phase alignment with the second EGRET pulse in the highest energy band of 16-30 keV. The average pulse spectrum joins smoothly to the high energy spectrum of OSSE, COMPTEL and EGRET, although the spectrum of Peak 1 is significantly harder than that of Peak 2. A break or turnover in the spectrum around 50 keV, previously suggested by OSSE data, is now clearly defined. The RXTE spectrum falls several orders of magnitude below the ROSAT emission in the 0.1 - 2 keV band, suggesting a thermal origin for the ROSAT pulse.

*Subject headings:* X-Rays: stars – stars: pulsars: individual (Vela Pulsar)

---

<sup>1</sup>E-mail: strickman@osse.nrl.navy.mil

## 1. Introduction

The Vela Pulsar (PSR B0833-45) is representative of a group of pulsars, with ages in the range  $\sim 10^4 - 10^5$  years, that are surrounded by synchrotron nebulae. Of these, the Vela Pulsar, PSR B1706-44, PSR B1951+32 and possibly PSR B0656+14 are also high energy  $\gamma$ -ray emitters (Thompson et al. thomp97 1997). In addition to these four pulsars, a number of other “Vela-type” pulsars have been observed to be steady point sources of soft X-rays (Becker & Trümper & becke97 1997). Because of its proximity and low spin-down age within this group, the Vela Pulsar is the easiest to observe across the high energy spectrum, being the brightest object in the sky above 100 MeV. Vela, as well as PSR B0656+14, exhibit soft (less than 1.2 keV) X-ray pulsations, detected by ROSAT (Ögelman ogelm93 1993). Recent observations of Vela by the OSSE (Strickman et al. stric96 1996) and COMPTEL (Bennett et al. benne94 1994) experiments on board Compton Gamma Ray Observatory have filled in part of the gap between soft X-rays and high energy  $\gamma$ -rays, extending the pulsed spectrum down to 50 keV. However, the 2-50 keV hard X-ray band has remained without a detection of pulsed emission.

Characterizing the pulsed emission in the 2-50 keV range is important for several reasons. The pulsed X-ray flux detected by ROSAT was extremely soft and well described by a black body model. Since the pulsed spectra above 50 keV are clearly nonthermal, measurements in the intervening energy band are required in order to determine the nature of the transition from a dominant thermal to nonthermal emission mechanism. In addition, the pulse profile above 50 keV is similar to that observed above 100 MeV, while the pulse profile in the black body region below 1.2 keV is significantly different. Determination of the pulsar profile in the 2 - 50 keV band is clearly also of interest. Finally, both polar cap (e.g. Daugherty & Harding daugh96 1996, Harding & Daughertyhard99 1999) and outer gap (e.g. Romani & Yadigaroglu roman95 1995, Romani roman96 1996) models make distinct predictions concerning spectra and pulse profiles in this energy region. Hence, 2 - 50 keV observations there may constrain one or both model categories.

In order to address this hole in spectral coverage, we have performed a sensitive Vela pulsar observation using the Proportional Counter Array (PCA) ex-

periment on board the Rossi X-ray Timing Explorer (RXTE; see Bradt, Rothschild & Swank bradt93 1993 for a description). In this paper, we report on the results of this observation, and discuss some of their implications for the questions mentioned above. Detailed comparisons with model predictions will be presented in a future paper (but see Harding & Daughertyhard99 1999).

## 2. Observations and Analysis

We observed the Vela Pulsar with RXTE during the intervals indicated in Table 1, with a total good exposure of 93 ksec. PCA data were collected in GoodXenon event-by-event mode and hence were available with full time and energy resolution. For a pulsar ephemeris, we used the Princeton Pulsar Database (Arzoumanian et al. arzou92 1992), which is available via the WWW at <http://pulsar.princeton.edu/ftp/gro/psrtime.dat>. For our analysis, we used the entry valid from MJD 50402 – 50479. Table 2 lists the frequency and derivatives from the database, in addition to “ $t_{0\text{geo}}$ ,” the absolute time epoch. The latter includes the Vela Pulsar correction of 13.4 msec, which accounts for variations in dispersion measure and in the definition of “pulse peak.” See the database web site for a detailed discussion of “ $t_{0\text{geo}}$ .”

Epoch folding analysis was accomplished using pre-release versions of the FASEBIN family of tools included in the FTOOLS version 4 release. These tools perform the actual phase coherent epoch fold (FASEBIN), add individual days together (FBADD), subtract “off-pulse” regions (FBSUB), and create light curves (FBSSUM) and phase-resolved spectra (FBFSUM). Subsequent analyses were performed using XSPEC and IDL. We have examined the time averaged light curves and phase resolved spectra, the variations in the time averaged light curve features with energy, and have looked for temporal variability in both flux and spectral shape.

In order to study the time averaged light curve as a function of energy, we folded the event stream into 88-bin (approximately 1 msec/bin) phase histograms which represent average light curves for each of three broad energy bands: 2 – 8 keV, 8 – 16 keV and 16 – 30 keV. The results are shown in Figure 1, where the origin of the phase axis represents the centroid of the radio peak. In the lowest band, we used layer 1 of the proportional counter only, while in the other bands

we used all three xenon layers summed together. The light curves have been divided into five phase regions, as listed in Table 3. The regions, entitled “Peak 1 Precursor”, “Peak 1”, “Peak 2”, “Off Pulse 1” and “Off Pulse 2” and abbreviated on the figure, were chosen by eye to assure that changes in peak shape with energy would not cause the “off pulse” regions to become contaminated with peak flux at any energy. In all cases, “peak 1” and “peak 2” refer to the order of the peaks as they follow the radio peak. We have examined smaller regions but have found that the statistical precision of the data do not support smaller regions than the ones used here. Regions OP1 and OP2, the two regions identified as “off-pulse,” were chosen as such since they are consistent with the light curve minimum, despite the fact that the EGRET result indicates that at gamma-ray energies there is modulated flux in the OP1 phase region.

To better characterize the behavior of light curve features with energy, we modeled the light curve using a constant background and two Lorentzian-shaped peaks. As we were primarily interested in peak width and separation, and due to limited statistics, the model did not include the peak 1 precursor region, and that region was excluded from the fits. This model represents the 2 – 8 keV and 8 – 16 keV data quite well (reduced  $\chi^2$  of 1.11 and 1.16 for 58 degrees of freedom respectively). In the 16 – 30 keV band, bin-to-bin fluctuations result in a reduced  $\chi^2$  of 1.44 for 58 dof. However, the model is quite acceptable in this band if we fold the data into 44 phase bins rather than 88. The resulting fit parameters are essentially identical to those from the original 88-bin best fit model.

Phase resolved spectra were created using the straightforward “on pulse” minus “off pulse” technique, then time normalized to the average over the entire light curve. This normalization removes any bias that might be introduced by having to make the peak 2 phase region wider than necessary at any given energy. Spectra were kept in native PCA channels, with layer 1 only used for channels less than 8 keV and the sum of all 3 Xenon layers used above 8 keV. Analyses of these spectra were performed using XSPEC together with PCA responses produced with the standard FTOOLS.

Finally, we also performed analyses of the light curve and spectra on a day-by-day basis. These were performed similarly to the time-integrated analyses discussed above, except that poorer statistics limited

us to relatively crude studies of broad band pulsed flux and spectrum shape as a function of time.

### 3. Results

We detect pulsed emission in all three of the broad energy bands shown in Figure 1. Using the Maximum Likelihood Ratio (MLR) test of Li & Ma lima83 (1983), we have assessed the probability (expressed as a number of Gaussian sigmas) that each of three light curve features in each band is consistent with random fluctuations in the data. As indicated in Table 4, both peaks are significantly detected in all three bands. The peak 1 precursor region is significant (and, at that, only marginally), in the 2 – 8 keV band only. We find no significant pulsed emission above background in either the OP1 region (between the peaks) or the OP2 region (outside the peaks). The lack of pulsed emission in the OP1 region is in contrast to the EGRET detection of significant interpeak emission in the Vela pulsar profile above 30 MeV.

In order to examine the behavior of the light curve features with energy and to quantitatively compare them with similar features found in high energy gamma-rays, we fit Lorentzian-shaped peak models, discussed in the previous section, to the observed light curves in all three bands. Figure 2 shows the results of these fits. In the cases of peak 1 absolute phase and the widths of both peak 1 and peak 2, we see no evidence for variation of the parameter with energy. Additionally, the fitted parameter values are consistent with the same parameter observed by EGRET above 100 MeV (Kanbach et al. kanba94 1994), as shown by the dashed lines in the figure.

However, we do see evidence that the peak separation differs from that observed by EGRET, especially at low energies. In particular, the peaks appear to be significantly closer together at 2 – 8 keV than observed by EGRET. Above 8 keV, peak separations are consistent with those observed by EGRET. The reduced  $\chi^2$  for modeling the peak separation vs. energy by the mean PCA result averaged over all three bands is 2.9, which corresponds to a 5% probability of the result being produced randomly. Hence we cannot say conclusively that the separation varies from PCA data alone. However, comparing the PCA results to the EGRET peak separation yields a reduced  $\chi^2$  of 15.4 corresponding to a random probability of  $2 \times 10^{-7}$ , which is clearly significant. We therefore conclude from the combination of PCA and EGRET

results that the peak separation increases with increasing energy in the X-ray regime, although there is no statistically significant evidence for change above 8 keV.

Peak minus Off-Pulse spectra were created for the peak 1 precursor, peak 1 and peak 2 phase regions. Power-law with photoelectric absorption fits have been performed for each spectrum. Fits have used the XSPEC PEGPWRLW photon spectrum model with normalization set to 10 keV and the XSPEC WABS absorption model with a column density fixed at  $1 \times 10^{20}$  atoms-cm $^{-2}$ , based on ROSAT results (Ögelman ogelman931993). The resulting best fit photon power-law indices  $\alpha$  are: Peak 1 precursor,  $\alpha = 1.57 \pm 0.29$ ,  $\chi^2/dof = 1.35$ ; Peak 1,  $\alpha = 0.68 \pm 0.14$ ,  $\chi^2/dof = 1.19$ ; and Peak 2,  $\alpha = 1.17 \pm 0.12$ ,  $\chi^2/dof = 1.49$ . While this simple model does not represent the spectra perfectly (although some portion of  $\chi^2$  stems from known systematics in the PCA response), the resulting indices are representative of the relative hardness of each spectrum. Comparing these indices to their mean, we can reject the hypothesis that they are drawn from the same distribution at about the  $3\sigma$  level. The PCA peak 1 and peak 2 spectra (with channels summed together for clarity of display) are shown in the context of optical and other X-ray and gamma-ray observations in Figure 3. They clearly continue the hardening trend from higher to lower energies first observed by OSSE and COMPTEL.

We have also produced a time history of the pulsed emission on a day-by-day basis. We see marginal evidence that the total pulsed flux may have disappeared during the first observing day in the 2 – 8 keV band and during the sixth observing day in the 8 – 30 keV band. In the former case, the probability of such a variation being a random fluctuation, as determined by  $\chi^2$ , is  $6 \times 10^{-4}$ , while in the latter it is  $2 \times 10^{-3}$ . The probability of seeing two such fluctuations in 16 trials from randomly distributed data is  $10^{-5}$ . Statistics do not allow further subdivision into individual light curve components and/or shorter time intervals. We have examined a number of possible systematics that could have caused this phenomenon. In particular, because the off-pulse phase region is used as background, normal PCA background concerns for weak sources do not apply. We refolded the data with an alternative ephemeris (based on some but not all of the same radio data) and obtained the same result. In addition, the fact that pulsations are observed in some energy band on all days mitigates against epoch

folding problems. Likewise, we find no evidence for deadtime variations, which would effect all energies equally if they were present in any event. Due to limited statistics and continuing concerns over possible systematic effects, we cannot draw any firm conclusions about variability of pulsed emission from these results. However, we have recently completed a much deeper RXTE observation of the Vela Pulsar, and will carefully examine it for time variability on daily and other time scales. None of the existing pulsar models have addressed the question of high-energy flux variability on day to week timescales.

#### 4. Discussion

Our detection of pulsed emission in the range 2 – 30 keV from the Vela pulsar has succeeded in filling in the gap over the hard X-ray energy band and has important implications for the origin of the high energy emission and its connection to lower energy bands. The pulse profile measured by RXTE from 2 – 30 keV shows two peaks separated by 0.4 in phase, similar to the profile measured at high energies. Figure 4 shows the Vela pulse profiles at energies ranging from optical to high-energy  $\gamma$ -rays, including the RXTE profile averaged over the 2 – 8 keV energy band. The phase of the RXTE Peak 1 is the same as that of EGRET and OSSE, within errors. The Vela profile above 2 keV thus shows a very similar behavior to the Crab pulse profile, but does not, however, duplicate the phase alignment of the Crab at lower energies.

The spectra of Peaks 1 and 2 also join smoothly, within errors, to the higher energy spectrum of OSSE, COMPTEL and EGRET, indicating that the RXTE emission is a continuation of the non-thermal magnetospheric emission to lower energy. The RXTE spectrum, however, clearly indicates a break at around 50 keV, confirming a feature that was suggested by the low-energy OSSE points. Recent RXTE upper limits on pulsed emission from PSR B1706-44 (Ray et al. 1999) and from PSR B1951+32 (Cheng & Ho 1997) also require similar low-energy breaks or turnovers in the high-energy spectra of these pulsars. Such a low-energy flattening or turnover is predicted by the polar cap cascade model (Daugherty & Harding 1996; Harding & Daugherty 1999). In this model the synchrotron spectrum of the pair cascade will exhibit a turnover at the local cyclotron frequency, blueshifted by the relativistic motion of the pairs along the magnetic field lines by a factor  $\Gamma_{\pm} \sim 20$ . The energy of the turnover

is a strongly increasing function of local magnetic field strength and thus provides a measure of the height of the emission above the neutron star surface. In the case of Vela, a turnover at 50 keV would indicate that the polar cap cascade emission is occurring at a height of 2 stellar radii above the surface. The outer gap model spectrum of Romani (1996) has an index of about -1.3 in the RXTE range, but falls somewhat above the RXTE spectral points and does not predict a low energy cutoff or turnover. The model of Cheng & Zhang (1999), in which particles from an outer gap accelerator travel toward the neutron star surface emitting curvature radiation, produces a non-thermal hard X-ray component through synchrotron radiation from the ensuing pair cascade. However, the predicted spectrum, having index -1.9, is much softer than our measured RXTE spectra.

The fact that the RXTE spectrum joins smoothly to the OSSE spectrum and falls significantly below the ROSAT spectrum provides strong evidence for a thermal rather than non-thermal origin for the ROSAT emission. The RXTE and ROSAT pulse profiles (see Figure 4) are also very different, indicating separate origins for the emission. A thermal component would most likely come from the hot neutron star surface or polar cap. This would be at odds with the outer gap model of Romani & Yadigaroglu (1995), who interpret the ROSAT pulse as non-thermal emission originating in acceleration regions in the outer magnetosphere.

It is evident from Figure 3 that the averaged RXTE spectrum would extrapolate several orders of magnitude below the optical points. However, the spectrum of Peak 2 is significantly softer than that of Peak 1. The spectrum of Peak 2, disregarding the lowest energy point which has a large error bar, would extrapolate to within a factor of two of the optical points. It would then not connect to the OSSE spectrum and would be a separate, low-energy component. Although the evidence for such a separate component in the Vela spectrum at low energies is speculative at best from the spectral data alone, there is possibly additional evidence to support such a picture from the pulse profiles. Figure 4 shows that the RXTE Peak 2 maximum seems to line up with the optical peak 2. The weaker secondary maximum in RXTE Peak 2 is in phase with the OSSE and EGRET second peaks. The phase of Peak 2, as discussed in Section 3. and shown in Figure 1, appears to move higher with increasing energy. It is in phase alignment with

the second optical pulse in the lowest energy band of 2 - 8 keV and in phase alignment with the second EGRET pulse in the highest energy band of 16-30 keV. The RXTE pulse may in fact be a blend of high and low energy components having different spectra, which could create the illusion of a peak moving with energy. While analysis of the present data using such a model would not be conclusive, we shortly expect to obtain an additional 300 ks of Vela observations with RXTE which should clarify the picture.

Finally, we point out that the RXTE Peak 1 precursor seems to be in phase with the radio peak (at phase 0 in Figure 4). The Peak 1 precursor has the softest spectrum of any pulse profile component and has disappeared into the background in the high-energy RXTE band (see Figure 1). There is also a peak in the optical profiles as well as a very weak and formally insignificant peak in the ROSAT profile in this phase region. Correlated RXTE and radio observations, which we expect to complete in the near future, will explore this connection.

We would like to thank the staff of the RXTE Guest Observer Facility for invaluable aid in performing these analyses. In particular, Arnold Rots was extremely cooperative and helpful. This work was supported in part by the NASA/RXTE Guest Investigator program.

## REFERENCES

- arzou92 Arzoumanian, Z., Nice, D. & Taylor, J. H. 1992, GRO/radio timing data base, Princeton University
- becke97 Becker, W. & Trümper, J. 1997, *A&A*, 326, 682
- benne94 Bennett, K., et al. 1994, *ApJS*, 90, 823
- bradt93 Bradt, H. V., Rothschild, R. E. & Swank, J. H. 1993, *A&AS*, 97, 355
- cheng97 Cheng, K. S. & Ho, C. 1997, *ApJ*, 479, L125.
- cheng99 Cheng, K. S. & Zhang, L. 1999, *ApJ*, in press.
- daugh96 Daugherty, J. K. & Harding, A. K. 1996, *ApJ*, 458, 278.
- hard99 Harding, A. K. & Daugherty, J. K. 1999, in Proc. of 3rd Integral Workshop, in press.
- kanba94 Kanbach, G., et al. 1994, *A&A*, 289, 855
- lima83 Li,T. & Ma,Y. 1983, *ApJ*, 272, 317
- nasut97 Nasuti, F.P., Mignani, R.,Caraveo, P.A. & Bignami, G.F. 1997, *A&A*, 323, 839
- ogelm93Ögelman, H. 1993, in *Lives of Neutron Stars*, ed. M.A. Alpar et al. (Dordrecht: Kluwer), 101
- ray99 Ray, A., Harding, A. K. & Strickman, M. S. 1999, *ApJ*, 513, in press.
- roman96 Romani, R. W. 1996, *ApJ*, 470, 469
- roman95 Romani, R. W. & Yadigaroglu, I.-A. 1995, *ApJ*, 438, 314.
- schon94 Schönfelder, V. et al. 1994, paper presented at 17th Texas Symp. on Relativistic Astrophysics
- stric96 Strickman, M.S., Grove, J.E., Johnson, W.N., Kinzer, R.L., Kroeger, R.A., Kurfess, J.D., Grabelsky, D.A., Matz, S.M., Purcell, W.R. & Ulmer, M.P. 1996, *ApJ*, 460, 735
- thomp97 Thompson, D.J., Harding, A.K., Hermsen, W. & Ulmer, M.P. 1997 in *Proceedings of the Fourth Compton Symposium*, ed. Charles D. Dermer et al. (Woodbury, New York: American Institute of Physics), 39

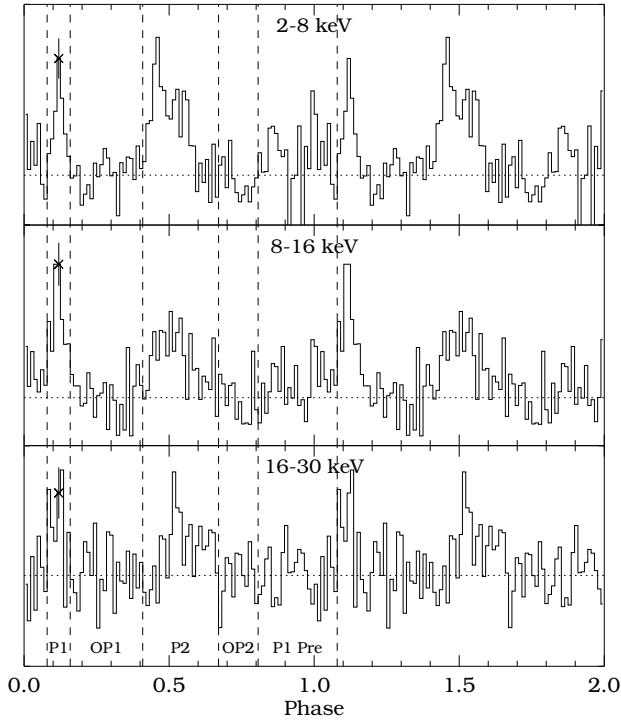


Fig. 1.— Vela pulsar phase histograms in several broad energy bands, averaged over the entire observation. The vertical scale is arbitrary, but the dotted line represents the average of the “off-pulse” regions. Each phase histogram displays a single representative error bar for that band. The phase region labels P1Pre, P1 and P2 refer to Peak 1 Precursor, Peak 1 and Peak 2 respectively. The regions OP1 and OP2 are the two “off pulse” regions.

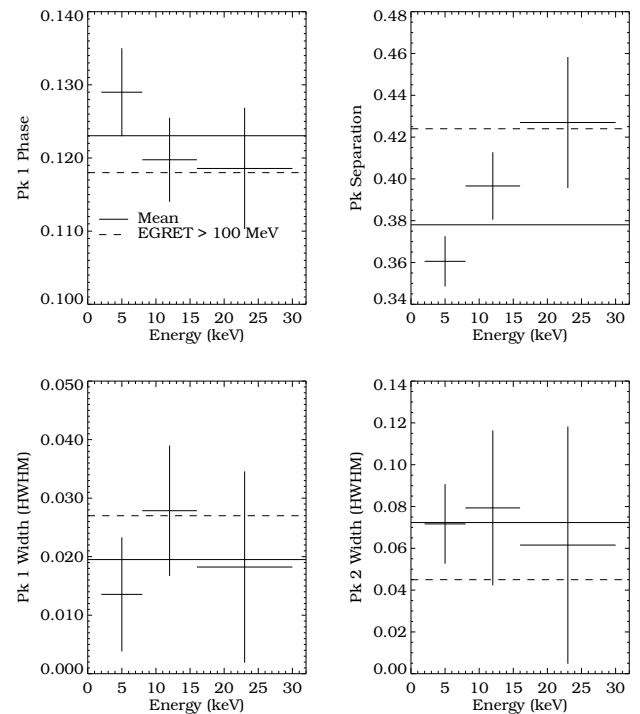


Fig. 2.— Light curve peak properties vs. energy. Parameters are determined by fitting a 2 Lorentzian peak model to the lightcurves for each PCA energy band. The solid line is the mean of the PCA results averaged over energy. The dashed line is the value of the same peak parameter above 100 MeV from EGRET (Kanbach et al. 1994).

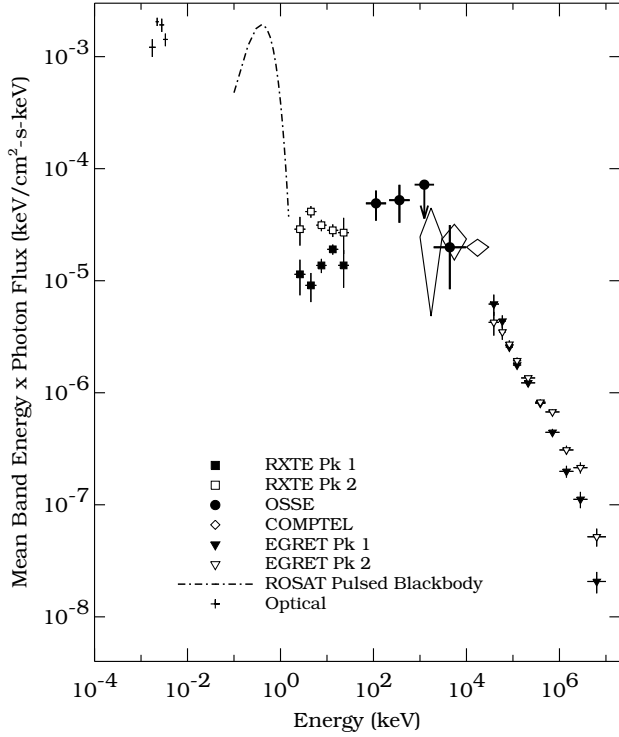


Fig. 3.— Energy spectrum of pulsed high-energy and optical emission from the Vela Pulsar. In addition to the PCA spectra from this work, data shown include results from optical (Nasuti et al. 1997), ROSAT (Ögelman 1993), OSSE (Strickman et al. 1996), COMPTEL (Schönfelder et al. 1994), and EGRET (Kanbach et al. 1994). All results but optical are pulsed flux averaged over the entire light curve. The optical points are total emission from the point source.

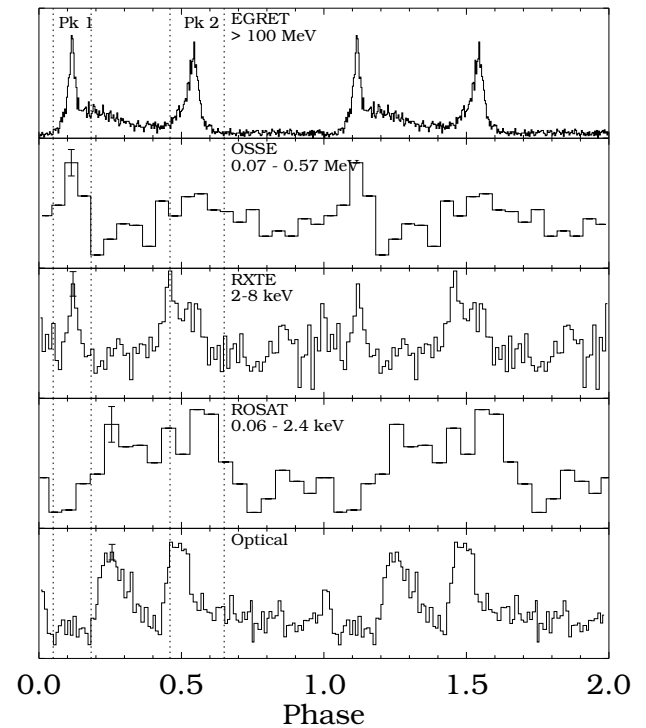


Fig. 4.— Epoch-folded light curves of pulsed high-energy and optical emission from the Vela Pulsar. In addition to the 2 - 8 keV PCA light curve from this work, data shown include results from EGRET, OSSE, ROSAT, and optical observations. See Figure 3 for references. In all cases, the origin of the phase axis is the phase of the centroid of the radio pulse.

Table 1: Vela Pulsar Observation Summary

StartTime (TJD)	Stop Time (TJD)	Exposure (ks)
50460.563	50460.643	4.4
50461.564	50461.692	7.2
50465.429	50465.761	17.7
50465.865	50465.984	5.4
50466.525	50466.657	6.6
50468.379	50468.649	11.7
50469.371	50469.731	16.8
50470.439	50470.736	14.8
50471.590	50471.740	8.4

Table 2: Vela Pulsar Ephemeris

$\nu$ (s <sup>-1</sup> )	11.1961237576948
$\dot{\nu}$ (s <sup>-2</sup> )	$-1.56671 \times 10^{-11}$
$\ddot{\nu}$ (s <sup>-3</sup> )	$3.27 \times 10^{-21}$
$t_{0\text{geo}}$ (MJD)	50440.000000226

Table 3: Peak and Off-pulse Phase Region Summary

Region	Start Phase	Phase Width
Peak 1 Precursor	0.807	0.272
Peak 1	0.079	0.080
Peak 2	0.409	0.262
Off-Pulse 1	0.159	0.250
Off-Pulse 2	0.671	0.136

Table 4: Vela Pulsar Maximum Likelihood Ratio (MLR) Test Summary

Energy Band	Peak 1 MLR $N_\sigma$	Peak 2 MLR $N_\sigma$	Peak 1 Precursor MLR $N_\sigma$
2 – 8 keV	6.7	8.9	3.5
8 – 16 keV	9.4	6.4	2.4
16 – 32 keV	5.0	3.7	0.2